

# RADIO CONTINUUM STUDY OF SUPERNOVA REMNANTS IN THE LARGE MAGELLANIC CLOUD – SNR J0519–6926

E.J. Crawford<sup>1</sup>, M.D. Filipović<sup>1</sup> and J.L. Payne<sup>2</sup>

<sup>1</sup>*School of Computing and Mathematics, University of Western Sydney  
Locked Bag 1797, Penrith South DC, NSW 1797, Australia*

<sup>2</sup>*Centre for Astronomy, James Cook University  
Townsville, QLD 4811, Australia*

(Received: February, 2008; Accepted: February, 2008)

**SUMMARY:** We present the results of new high resolution ATCA observations of SNR J0519–6926. We found that this SNR exhibits a typical “horseshoe” appearance with  $\alpha = -0.55 \pm 0.08$  and  $D = 28 \pm 1$  pc. No polarization (or magnetic fields) are detected to a level of 1%. This is probably due to a relatively poor sampling of the  $uv$  plane caused by observing in “snap-shot” mode.

**Key words.** ISM: supernova remnants – Magellanic Clouds – Radio Continuum: ISM – SNR B0520–69

## 1. INTRODUCTION

The study of radio supernova remnants (SNRs) in nearby galaxies is of major interest in order to understand the radio output of more distant galaxies and to understand the processes that occur on local interstellar scales within our own Galaxy. Unfortunately, the distances to many Galactic remnants are uncertain by a factor of 2, leading to a factor of 4 uncertainty in luminosity and of 5.5 in the calculated energy release of the initiating supernova (SN). At a distance of  $\sim 50$  kpc (Hilditch et al. 2005), the Large Magellanic Cloud (LMC) is one of the prime targets for the astrophysical research of galactic objects, including SNRs. This is because these remnants are located at a known distance, yet close enough to allow a detailed analysis of them.

SNRs reflect a major process in the elemental enrichment of the interstellar medium (ISM). Multiple supernova explosions close together generate super-bubbles typically hundreds of parsecs in extent. Both are among the prime drivers controlling the morphology and the evolution of the ISM. Their properties are therefore crucial for the full understanding of the galactic matter cycle.

Radio observations are commonly used to discover and characterize SNRs, as the non-thermal emission typical of SNRs is easily detectable at centimeter radio wavelengths. Verification may be based on a combination of radio spectral index, morphology, co-identifications in other domains (such as optical and/or X-ray), flux density and location within the galaxy under study. There are over 40 confirmed SNRs in the LMC and another 35-40 candidates (Payne et al. 2008).

SNR J0519–6926 was initially classified as an SNR based on the Einstein X-Ray survey by Long et al. (1981) (named LHG 27) and Wang et al. (1991) (named W 19). Mathewson et al. (1983) catalogued SNR J0519–6926 as B0520–69.4 based on their optical observations, reporting an estimated size of  $138'' \times 104''$ . Filipović et al. (1998) added further confirmation, with a set of radio continuum observations (with the Parkes telescope) on a wide frequency range. Blair et al. (2006) report detection at far ultraviolet (FUV) wavelengths. Haberl & Pietsch (1999) (named SNR as HP 915) and Williams et al. (1999) discuss the X-Ray properties of SNR J0519–6926 based on ROSAT observations. Most recently Payne et al. (2008) presented optical spectroscopy of a wide range of LMC SNRs including SNR J0519–6926. They found an enhanced  $[\text{SII}]/\text{H}\alpha$  ratio of 0.8 typical for SNRs.

## 2. OBSERVATION DATA

We observed SNR J0519–6926 with the Australia Telescope Compact Array (ATCA) on 6<sup>th</sup> April 1997, with array configuration 375-m, at wavelengths of 6 and 3 cm ( $\nu=4790$  and 8640 MHz). The observations were done in so called “snap-shot” mode, totaling  $\sim 1$  hour of integration over a 12 hour period. Source 1934–638 was used for primary calibration and source 0530–727 was used for secondary calibration. The MIRIAD (Sault & Killeen 2006) and KARMA (Gooch 2006) software packages were used for reduction and analysis. More information about observing procedure and another source (LMC SNR B0513–69) observed during this session can be found in Bojičić et al. (2007).

Images were prepared, cleaned and deconvolved using MIRIAD tasks. Baselines formed with the 6<sup>th</sup> ATCA antenna were excluded, as the other five antennas were arranged in a compact configuration. The 6 cm image (Fig. 1) has a resolution of  $32''$  and the r.m.s noise is estimated to be 0.4 mJy/beam. Similarly, the 3 cm image (Fig. 2) has a resolution of  $20''$  and the r.m.s noise is estimated to be 0.4 mJy/beam. A 3 cm image was also created with a resolution of  $32''$  to compliment the 6 cm image, and this was used in the preparation of Figs. 1 and 3.

## 3. RESULTS AND DISCUSSION

The remnant has a classical horseshoe morphology centered at  $\text{RA(J2000)}=5^{\text{h}}19^{\text{m}}45.3^{\text{s}}$ ,  $\text{DEC(J2000)}=-69^{\circ}26'00.6''$  with a nearly circular diameter of  $140'' \pm 5''$  ( $28 \pm 1$  pc). This is reasonably consistent with the optical size reported by Mathewson et al. (1983), and in agreement with the X-ray size  $156'' \times 132''$  reported by Williams et al. (1999).

Flux density measurements were made at 6 and 3 cm, resulting in values of 71.3 mJy and 43.5 mJy respectively (Table 1). We made our own measurement of flux density at 1400 MHz using the mosaic image described in Hughes et al. (2007). A spectral index (defined as  $S \propto \nu^\alpha$ ) was plotted using the flux densities in Table 1 (Fig. 4) and estimated to be  $\alpha=-0.55 \pm 0.08$ , which is typical for SNRs (Filipović et al. 1998). We note that there are two points (843 and 2300 MHz) which lie slightly off the line of best fit. The estimate of flux density for these points are very uncertain, and the error bars are probably too conservative. This is due to missing short spacings effects at 843 MHz. At 2300 MHz a large r.m.s noise coupled with a large Parkes beam size accounts for the errors. We also calculated a two point spectral index between 6 and 3 cm and found  $\alpha=-0.84$ . This is somewhat steeper than the overall  $\alpha=-0.55$  but also expected as for most SNRs the flux density is fading with increasing frequency.

From our spectral index map (Fig. 3) we can see that spectral index is changing rapidly at the SNR front shock with the usual  $\alpha \approx -0.8$ , due to the non-thermal nature of emission in the shocked regions. Further on, inside the SNR shell,  $\alpha$  tends to be flatter ( $-0.4 \leq \alpha \leq 0$ ) as the emission has larger thermal component. We note that there are two “holes” in the spectral index map (Fig. 3) were thermal emission ( $\alpha \geq 0$ ) from this SNR tends to dominate. Comparing our radio-continuum images with ROSAT HRI X-ray images of Williams et al. (1999; Fig. 11) shows an anti-correlation between radio and X-ray emission.

Linear polarization images for each frequency were created using  $Q$  and  $U$  parameters. While we detect no reliable polarization at 8640 MHz, the 4790 MHz image reveals some very low level linear polarization. Without reliable polarization measurements at the second frequency we could not determine if any Faraday rotation was present.

The mean fractional polarization at 4790 MHz was calculated using flux density and polarization:

$$P = \frac{\sqrt{S_Q^2 + S_U^2}}{S_I} \cdot 100\% \quad (1)$$

where  $S_Q$ ,  $S_U$  and  $S_I$  are integrated intensities for  $Q$ ,  $U$  and  $I$  Stokes parameters. Our estimated value is  $P \cong 1\%$ .

## 4. CONCLUSION

We conducted the highest resolution observations to date of SNR J0519–6926. From these observations we found a diameter of  $140'' \pm 5''$ , a spectral index  $\alpha=-0.55 \pm 0.08$  and no linear polarization to a level of  $\sim 1\%$ .

**Table 1.** Integrated Flux.

	$S_I$ (408 MHz)	$S_I$ (843 MHz)	$S_I$ (1400 MHz)	$S_I$ (2300 MHz)	$S_I$ (4790 MHz)	$S_I$ (8640 MHz)
SNR J0519–6926	280 mJy	141 mJy	135 mJy	124 mJy	71.3 mJy	43.5 mJy
Reference	Clarke et al. 1976	Mills et al. 1984	This Work	Filipović et al. 1996	This Work	This Work

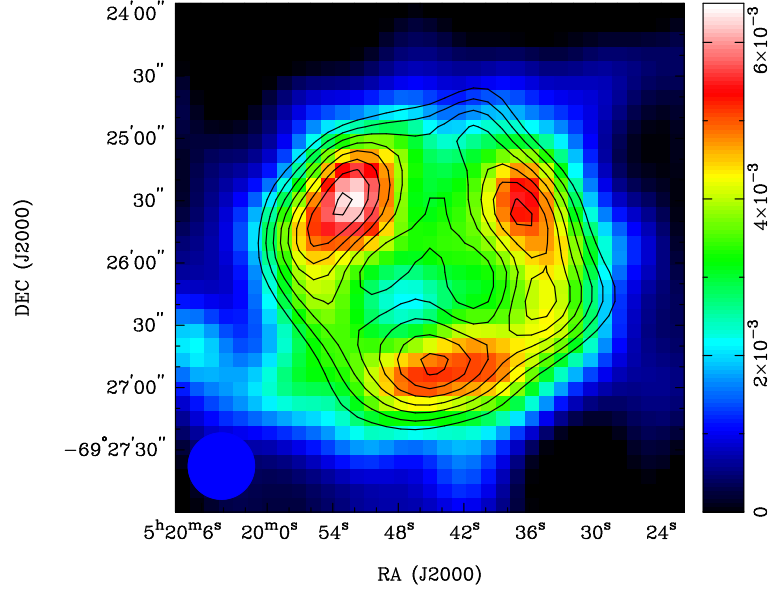


**Fig. 1.** ATCA observations of SNR J0519–6926 at 6 cm (4790 MHz) overlaid with 3 cm (8640 MHz) complimentary resolution contours. The contours are from 1.2 to 4 mJy/beam in 0.4 mJy/beam steps. The blue circle in the lower left corner represents the primary beam of 32". The sidebar quantifies the pixel map and it's units are mJy/beam.

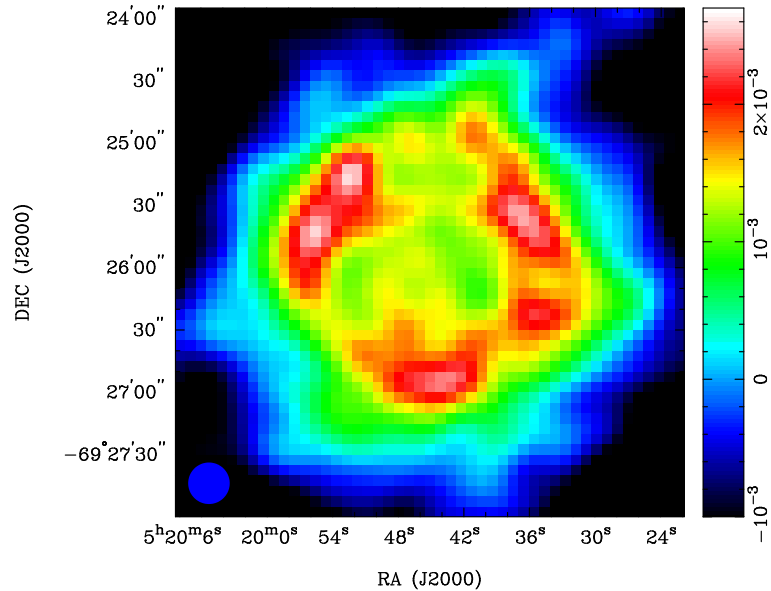


**Fig. 2.** ATCA 3cm observations of SNR J0519–6926. The blue circle in the lower left corner represents the 3 cm (8640 MHz) primary beam of 20". The sidebar quantifies the pixel map and it's units are mJy/beam.

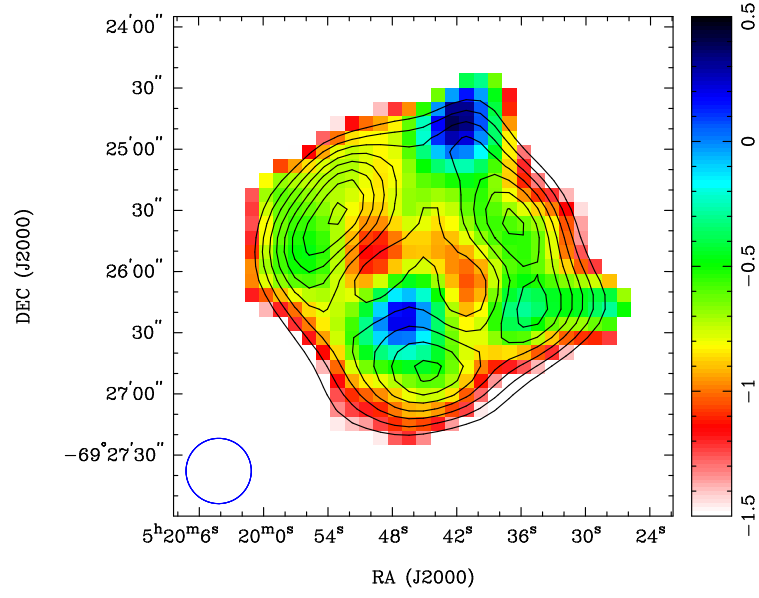


**Fig. 3.** *Spectral index map of SNR J0519-6926 overlaid with 3 cm (8640 MHz) contours. The contours are from 1.2 to 4 mJy/beam in 0.4 mJy/beam steps. The blue circle in the lower left corner represents the primary beam of 32". The sidebar quantifies the pixel map, representing the spectral index.*

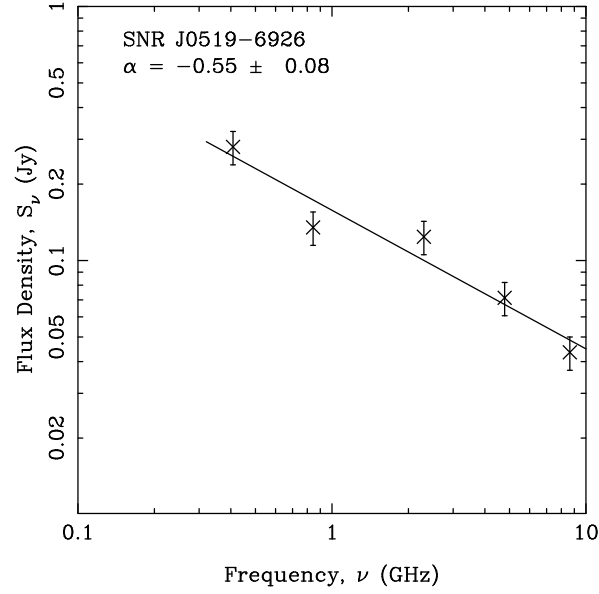


**Fig. 4.** *Radio Spectrum of SNR J0519-6926*

*Acknowledgements* – We used the KARMA software package developed by the ATNF. The Australia Telescope Compact Array is part of the Australia Telescope which is funded by the Commonwealth of Australia for operation as a National Facility managed by CSIRO.

## REFERENCES

- Blair, W. P., Ghavamian, P., Sankrit, R., Danforth, C. W.: 2006, *Astron. Astrophys. Suppl. Ser.*, **165**, 480
- Bojičić, I. S., Filipović, M. D., Parker, Q. A., Payne, J. L., Jones, P. A., Reid, W., Kawamura, A., Fukui, Y. 2007, *Mon. Not. R. Astron. Soc.*, **378**, 1237
- Clarke, J. N., Little, A. G., Mills, B. Y.: 1976, *Aust. J. Phys. Astrophys. Suppl.*, **40**, 1
- Filipović, M. D., White, G. L., Haynes, R. F., Jones, P. A., Meinert, D., Wielebinski, R., Klein, U.: 1996, *Astron. Astrophys. Suppl. Ser.*, **120**, 77
- Filipović, M. D., Haynes, R. F., White, G. L., Jones, P. A.: 1998, *Astron. Astrophys. Suppl. Ser.*, **130**, 421
- Gooch, R.: 2006, Karma Users Manual, ATNF
- Haberl, F., Pietsch, W.: 1999, *Astron. Astrophys. Suppl. Ser.*, **139**, 277
- Hilditch, R. W., Howarth, I. D., Harries, T. J.: 2005, *Mon. Not. R. Astron. Soc.*, **357**, 304
- Hughes, A., Staveley-Smith, L., Kim, S., Wolleben, M., Filipović, M. 2007, *Mon. Not. R. Astron. Soc.*, **382**, 543
- Long, K. S., Helfand, D. J., Grabelski, D. A.: 1981, *ApJ*, **248**, 925
- Mathewson, D. S., Ford, V. L., Dopita, M. A., Tuohy, I. R., Long, K. S., Helfand, D. J.: 1983, *Astron. Astrophys. Suppl. Ser.*, **51**, 345
- Mills, B. Y., Turtle, A. J., Little, A. G., Durdin, J. M.: 1984, *Aust. J. Phys.*, **37**, 321
- Payne, J. L., White, G. L., Filipović, M. D. 2008, *Mon. Not. R. Astron. Soc.*, **383**, 1175
- Sault, R., Killeen, N.: 2006, Miriad Users Guide, ATNF
- Wang, Q., Hamilton, T., Helfand, D. J., Wu X.: 1991, *ApJ*, **374**, 475
- Williams, R. M., Chu, Y.-H., Dickel, J. R., Petre, R., Smith, R. C., Tavarez, M.: 1999, *Astron. Astrophys. Suppl. Ser.*, **123**, 467

## RADIO KONTINUM STUDIJA OSTATKA SUPERNOVE U VELIKOM MAGELANOVOM OBLAKU – SNR J0519–6926

E.J. Crawford<sup>1</sup>, M.D. Filipović<sup>1</sup> and J.L. Payne<sup>2</sup>

<sup>1</sup>*School of Computing and Mathematics, University of Western Sydney  
Locked Bag 1797, Penrith South DC, NSW 1797, Australia*

<sup>2</sup>*Centre for Astronomy, James Cook University  
Townsville, QLD 4811, Australia*

У овој студији представљамо нове АТЦА радио-континуум резултате високе резолуције посматрања остатка супернове (ОСН) у Великом Магелановом Облаку – SNR J0519–6926. Нашли смо да овај ОСН има типичну морфологију (потковица) за ову врсту објеката са радио спектралним индексом

од  $\alpha = -0.55 \pm 0.08$  и дијаметром од  $D = 28 \pm 1$  парсека. Нисмо детектовали поларизацију (ни магнетно поље) до нивоа од 1%. Разлог за не постојање поларизације у нашим посматрањима треба тражити у техници ових посматрања која су обављена у тзв. “снап-шот” моду који је покрио само мањи део  $uv$  поља.